Design and Analysis of a Novel X-Y Table

J.F. PAN[1] N.C. CHEUNG[2] Guangzhong CAO[1] Hong QIU[1]

[1]College of Mechatronics and Control Engineering, Shenzhen University, Shenzhen, P.R.China,
E-mail:gzcao@szu.edu.cn
[2]Department of EE, The Hong Kong Polytechnic University, Hong Kong,
E-mail: norbert.cheung@polyu.edu.hk

Abstract—A novel X-Y table based on linear switched reluctance principle is proposed in this paper. The proposed direct-drive actuator has the characteristics of low cost, simple mechanical structure and high reliability. Finite element analysis (FEA) proves that the phases between any of the linear motors of the X-Y table are decoupled and each phase can be controlled independently. Experimental results verify that the motion control system based on the X-Y table has good dynamic characteristics.

Keywords-switched reluctance, direct-drive, FEA

I. INTRODUCTION

In most advanced manufacturing processes, two-dimensional motions are in high demand for industrial applications such as parts assembly, component insertion, machining, etc. A traditional X-Y table often utilizes a rotary motor and couples its output shaft to mechanical translators such as gears or bears to perform linear motion; by vertical arrangement of two such linear motion implementations, two-dimensional movement is achieved. In a direct-drive system, the mechanical output is directly generated to the actuator and load and it has the characteristics of high force density, high precision and low production cost [1]. By elimination of mechanical transmissions, such as rotary-to-linear couplers, the control object, together with the actuator can be implemented as an integral system, which is capable of fast response, high flexibility and can have a simple structure.

The X-Y table based on direct-drive idea can be constructed according to different motor methodologies such as a pair of linear direct current motors (LDCM), linear induction motors (LIM), linear permanent magnetic motors (LPMM) or linear switched reluctance motors (LSRM), etc. Due to the presence of a commutator, the LDCM requires frequent adjustment and maintenance. The principle of the LIM is similar to a common rotary induction motor with a robust structure. Though linear motion of high speed or high-precision is difficult to achieve due to the low air gap flux density [2], a variety of applications can still be found for a long-stroke motion such as the magnetic levitation train for railway transportation [3]. The LPMM is the only type of linear actuator available to industry by present and it has the advantages of wide range of speed regulation capability and stable output performance. One structural disadvantage of such linear motor is the utilization of expensive rare-earth permanent magnets to achieve better performance and efficiency. Due to the characteristics of the permanent magnets, a LPMM is not suitable under hostile environment that has a various temperature change. Moreover the overall cost of the linear motion system is high.

II. DESIGN AND CONSTRUCTION OF THE X-Y TABLE

With fast advancement of power electronics technology, research on switched reluctance motors becomes more and more extensive. A typical SR machine has the following characteristics,

- The mechanical structure is simple and robust with doubly-salient stator. The motor can operate under various hostile environments with large temperature difference since no permanent magnets or commutator involved.
- Since the winding is fixed only on the stator, the motor is easy for cooling and has low heat loss thus it has high efficiency.
- Torque generation is irrelevant of current directions. Therefore the drive topology can be minimized to reduce system cost.

According to the winding arrangement, a LSRM can be categorized as "active-stator-passive-translator" and "passive-stator-active-translator" structure [4]. The motion system applies the "passive-stator-active-translator" scheme for the following reasons,

- Simple manufacture of the stator base with no complicated coil arrays
- Flexible traveling range and stator dimensions
- Easy manufacture of mover slots with mounted coil windings
- Low overall production cost

Based on the idea of "passive stator-active translator" structure, the linear motor is constructed as shown in Fig.1. The motor is composed of the moving platform and the stator base. The stator base is made of aluminum alloy to minimize the mass and facilitate the magnetic flux path. A pair of high-grade linear guides is fixed on the stator base to facilitate the movement of the moving platform. The stator utilizes 0.5mm thick silicon-steel plates with tooth structure instead of any expensive materials such as rare-earth permanent magnets. A pair of aluminum locking bars is fixed on the stator base slot to hold the plates. The moving platform is composed of three-phase movers with coils. Locking pins are used to fix the mover plates.

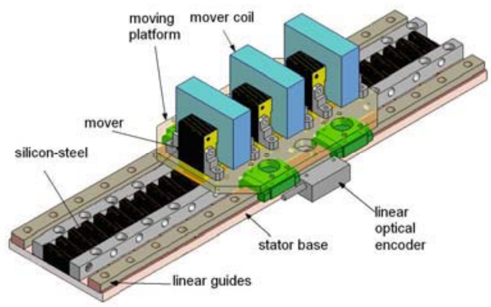

(a)

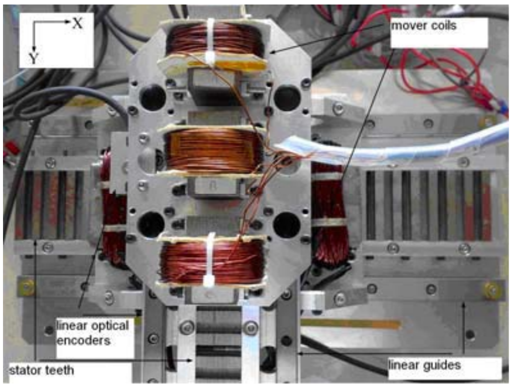

(b)

Fig. 1: The LSRM (a) and the X-Y table (b)

Similar to the structure of a typical 6/4 rotary SR motor, each phase of the three phases is separated by 120° electrically, which is 1+2/3 pitch distance, i.e. 10mm. The pitch distance is preferred to be 12mm to avoid any rounding error from 5/3 pitch distance. The features of the mover structure can be summarized as the following,

- The decoupled flux windings lead to a simpler motor model due to zero mutual inductance.
- The individual phase windings reduce the manufacturing cost and complexity.
- Long travel distance can be accomplished easily by combining longitudinal track guides.

The construction of the X-Y table is based on vertical stacking of such two LSRMs to facilitate two-dimensional movement as shown in Fig.1 (b). Since the X motor moves with the Y motor simultaneously, the X platform has a wider mover and stator tooth structure to generate larger propulsion forces. Table 1 shows mechanical and electrical parameters of the X-Y table.

Table 1: Mechanical and electrical parameters

Mass of X moving platform（not including Y platform）	2.8 Kg
Mass of Y moving platform	1.5 Kg
Stroke of X moving platform	170 mm
Stroke of X moving platform	120 mm
Width of X moving platform	50 mm
Width of Y moving platform	24 mm
Air gap of X moving platform	0.3 mm
Air gap of Y moving platform	0.2 mm
Pole-pitch	12 mm
Tooth width	6 mm
Encoder resolution	1 µm

III. MATHEMATICAL MODEL OF THE X-Y TABLE

Since the X and Y table is magnetically decoupled, for any direction of movement, the equations that governs the voltage balance relationship of the LSRM can be described as the following,

$$V_k = R_k i_k + \frac{\partial \lambda_k(i_k, x)}{\partial x}\frac{dx}{dt} + \frac{\partial \lambda_k(i_k, x)}{\partial i_k}\frac{di_k}{dt} \quad (1)$$

where V_k ， i_k and R_k are winding voltage, current and resistance. $x(t)$ is relative position from the mover to the stator and λ_k is flux-linkage.

The force balance equation can be described as the following for any direction of movement as,

$$f_{x(y)}(i_a(t), i_b(t), i_c(t), x(t)) = \sum_{k=a}^{c} \frac{\partial \int_0^{i_k(t)} \lambda_k \cdot d\tau_k(t)}{\partial x(t)} \quad (2)$$

$$= \sum_{k=a}^{c} f_k(i_k(t), x(t)) = M_m \frac{d^2x(t)}{dt^2} + B_v \frac{dx(t)}{dt} + f_l(t)$$

where $f_{x(y)}$ is generated electromagnetic force, $f_l(t)$ is the load force, M_m and B_v are mass and friction coefficient, respectively.

For any phase of X or Y table, inductance can be approximately represented by Fourier Series Expansions as [4],

$$L_a = L_{ls} + L_o + L_\Delta \cos(\frac{2\pi s_{x(y)}}{p}) \quad (3)$$

$$L_b = L_{ls} + L_o + L_\Delta \cos(\frac{2\pi s_{x(y)} - \frac{2}{3}\pi p)}{p}) \quad (4)$$

$$L_c = L_{ls} + L_o + L_\Delta \cos(\frac{2\pi s_{x(y)} - \frac{4}{3}\pi p)}{p}) \quad (5)$$

where $L_o = \frac{\mu_0 d^2 N^2}{z} \cdot \frac{p-q}{p}$ and $L_\Delta \approx \frac{\mu_0 d^2 N^2}{z} \cdot \frac{q}{p}$, L_{ls} is leakage inductance.

IV. SIMULATION ANALYSIS OF THE X-Y TABLE

The purpose of finite element analysis for the X-Y table is to verify that the coupling effect between any two phases can be neglected for each direction of movement, so that each phase of the LSRM can be controlled independently. Further FEA is conducted for the prediction of motor performance such as force output capability.

A. Analysis of coupling effect

Three-dimensional FEA is carried out for the test of phase coupling effect. Any one phase of the three phases from X or Y table is excited with a DC current such as 10A. By the inspection of the magnetic flux distribution from other two phases, the coupling effect can be explored. As shown in Fig.2 (a), the magnetic flux mainly distribute among the excited mover, the air gap and the stator. From Fig.2 (b) and (c), by exploring from the magnetic flux of mover cross section, it can be concluded that the induced flux value diminishes as the relative position to the excited mover increases. Since the absolute induced value is about a thousandth of the excited value, the coupling effect can be neglected.

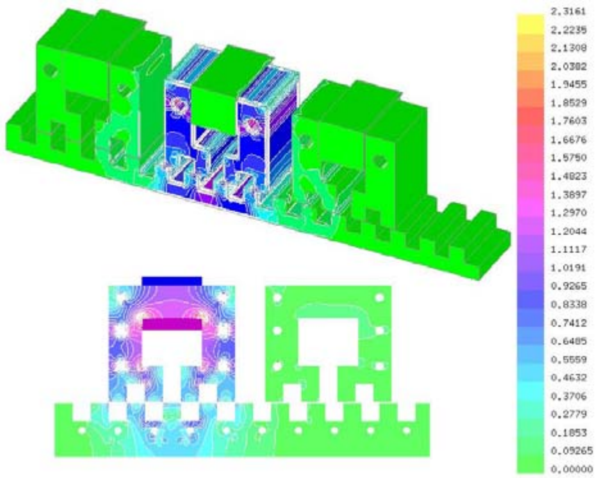

(a)

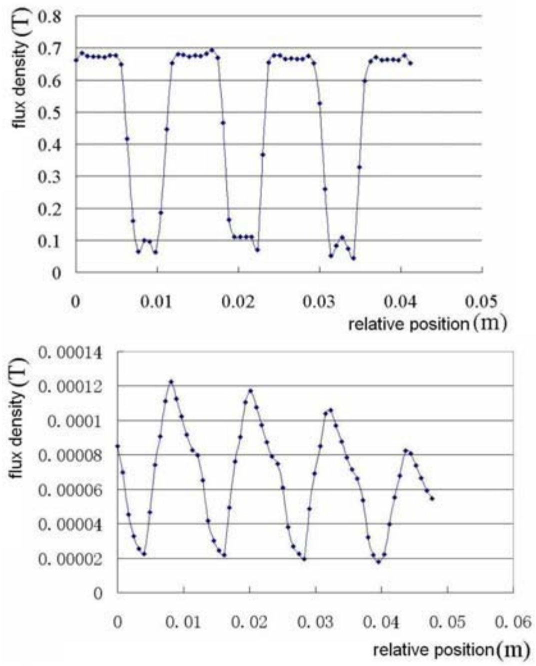

(b)

Fig. 2: FEA results of coupling effect—(a) flux contour (b) flux distribution in the excited and adjacent phase

B. Analysis of force output

The simulation results of the propulsion force are shown in Fig.3 for X and Y table respectively. Since X table has relatively larger air gap and moving mass, the force value of X table is comparably low of Y table.

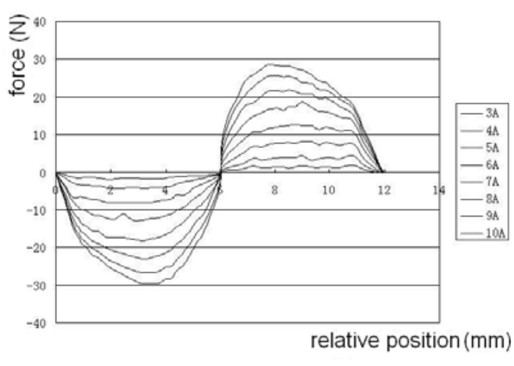

(a)

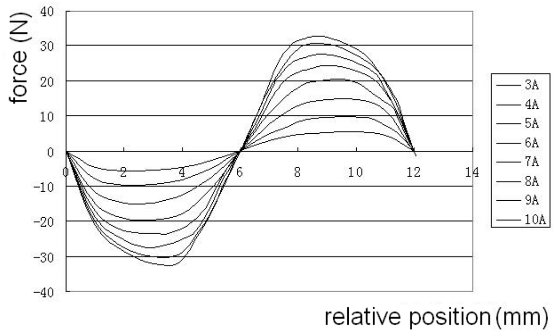

(b)

Fig. 3: Propulsion force output of (a) X table and (b) Y table

V. EXPERIMENTAL RESULTS

Since force, current and position have nonlinear relationship for a LSRM, a proper linearization scheme is required before the implementation of any control algorithm. To optimize between computation efficiency and memory consumption, a pair of low-resolution two-dimensional look-up tables are employed for each axis of movement with linear interpolation to calculate the intermediate values [5]. Since force, current and position are related in three dimensions, a 2D force-current-position look-up table for each axis is sufficient to describe the nonlinear force profile. The experiment to find out the inverse relationship between current, force and position has been conducted. By fixing the moving platform of each table at corresponding positions within one pole width, currents are measured for the generation of the desired force. Alternatively, the look-up tables are generated from the inverse function of force versus current and position. The generated 27×27-matrix is employed to build up the look-up tables for each axis of motion and sufficient to describe the force profile within the error of 5% [5].

The experiment is implemented on a dSPACE DS1104 DSP motion controller card. This card has an on-board 250MHz DSP for real-time computation and it interfaces with the PC through the PCI bus. It consists of two channels of 24-bits incremental encoder inputs, six channels of 12-bit analog input and six channels 12-bit analog output. The control card can directly interface with Real-Time Workshop and MATLAB and control parameters can be modified online. The overall control block diagram is shown in Fig.4 with a sampling rate of 10 KHz for the inner current loop and 2KHz for the outer position loop.

The step position responses of each moving platform are recorded as the results shown in Fig.4. Since the moving platform of X table moves simultaneously with Y table, it can be concluded from the step responses that the X moving platform has a relatively larger overshoot and longer rising time compared with that of the Y moving platform.

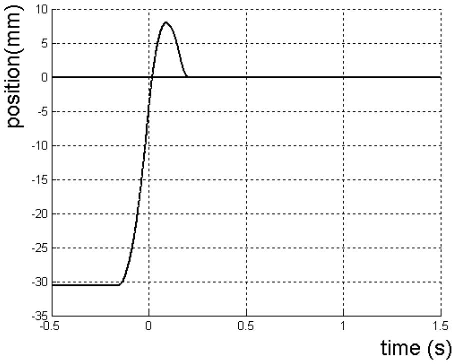

(a)

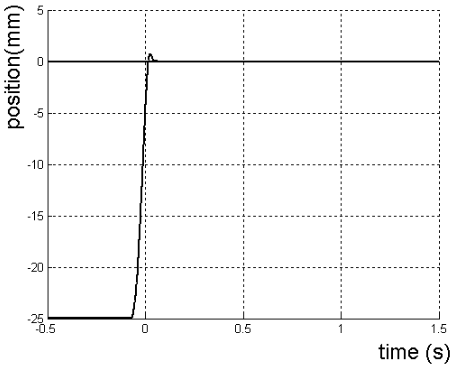

(b)

Fig. 4: Step response of (a) X table and (b) Y table

The dynamic responses of sine and cosine curves as the position commands can be found as shown in Fig.5. The tracking profiles show that each axis of motion is capable of following the command signal precisely. The command signal and response almost overlap for both axes as shown in Fig.5 (a) and (b). The error dynamics can be found in Fig.5 (c) and (d). The absolute errors fall within 0.35 mm, 3% of the total range (11.5 mm). It is clear that for both diagrams, the errors for opposite directions are not identical in each axis of motion. This is because the mechanical structures in both axes are not uniform such that the motor experiences unbalanced frictions at different positions.

From the experimental results, the position controllers are capable of correction for such imperfections that exist in mechanical manufacture and the simple PID controller ensures the implementation for future industrial applications of the X-Y table.

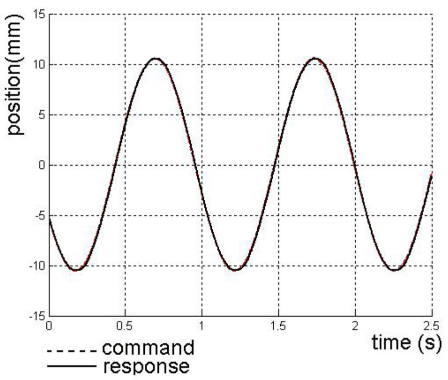

(a)

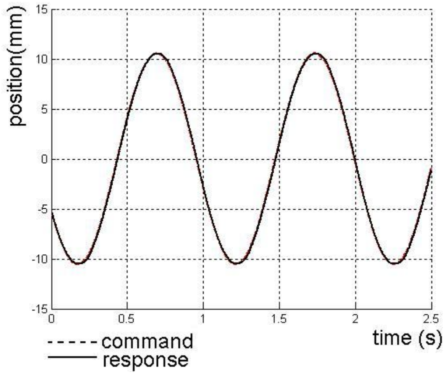

(b)

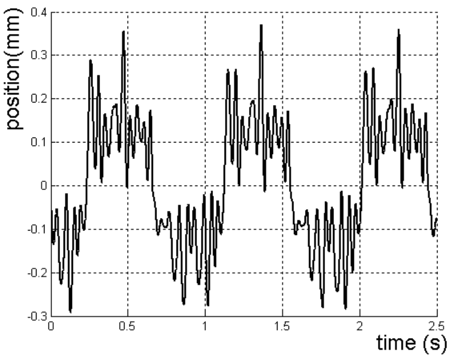

(c)

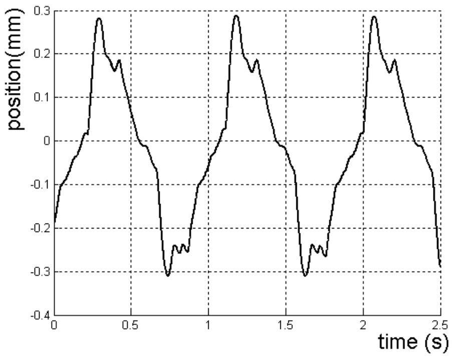

(d)

Fig. 5: Position response (a) X table, (b) Y table and error response of the X-Y table (c) X table, (d) Y table

The dynamic tracking profile of circle and line are demonstrated in Fig. 6 (a) and (b) respectively.

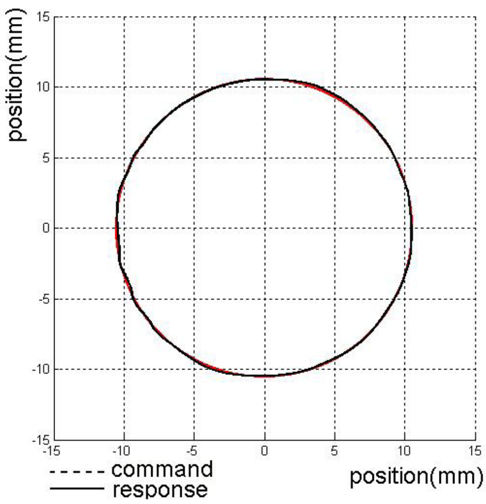

(a)

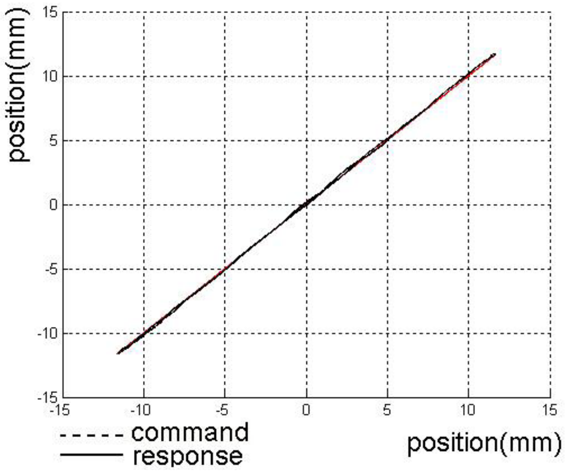

(b)

Fig. 6: The tracking response from the X-Y table of (a) circle and (b) straight line

VI. CONCLUSIONS

A novel small-size X-Y table based on switched reluctance principle is proposed in the paper. This X-Y table has the characteristics of simple and robust structure, low manufacturing cost and high reliability. Preliminary simulation and experimental results show that the motion control system has good dynamic performance and it is expected the proposed X-Y table to be an ideal replacement for traditional X-Y tables in industrial automation applications.

ACKNOWLEGEMENT

Project 200734 supported by SZU R/D Fund

REFERENCES

[1] I. Boldea and S. A. Nasar, “Linear Electric Actuators and Generators”, Cambridge University Press, London, UK, 1997.

[2] Jacek F. Gieras and Zbigniew J. Piech, “Linear synchronous motors—transportation and automation systems”, Boca Raton, Fla., CRC Press, 2000.

[3] R. Krishnan, “Switched Reluctance Motor Drives: Modeling, Simulation, Analysis, Design, and Applications”, Boca Raton, FL : CRC Press, 2001.

[4] C. T. Liu, L. F. Chen, J. L. Kuo, Y. N. Chen, Y. J. Lee, and C. T. Leu, “Microcomputer Control Implementation of Transverse Flux Linear Switched Reluctance Machine with Rule-based Compensator,” IEEE Trans. Energy Conversion, vol. 11, pp. 70–75, Mar. 1996.

[5] J.F. Pan, San Chin Kwok, Norbert C. Cheung and J.M. Yang, “Auto Disturbance Rejection Speed Control of a Linear Switched Reluctance motor”, Fortieth International IAS Annual Meeting, Industry Applications Conference, 2005, Volume 4, 2-6 Oct. 2005 Page(s):2491 - 2497 Vol. 4.